

Supplementary Materials for:  
Orders of magnitude reduction in the thermal conductivity of polycrystalline  
diamond through carbon, nitrogen, and oxygen ion implantation

Ethan A. Scott<sup>a</sup>, Khalid Hattar<sup>b</sup>, Jeffrey L. Braun<sup>a</sup>, Christina M. Rost<sup>a</sup>, John T. Gaskins<sup>a</sup>, Tingyu Bai<sup>c</sup>, Yekan Wang<sup>c</sup>,  
Claire Ganski<sup>c</sup>, Mark Goorsky<sup>c</sup>, Patrick E. Hopkins<sup>a,d,e,\*</sup>

<sup>a</sup>*Department of Mechanical and Aerospace Engineering, University of Virginia, Charlottesville, Virginia 22904, USA*

<sup>b</sup>*Sandia National Laboratories, Albuquerque, New Mexico 87185, USA*

<sup>c</sup>*Materials Science and Engineering, University of California Los Angeles, Los Angeles, California 90095, USA*

<sup>d</sup>*Department of Material Science and Engineering, University of Virginia, Charlottesville, Virginia 22904, USA*

<sup>e</sup>*Department of Physics, University of Virginia, Charlottesville, Virginia 22904, USA*

---

---

---

\*Principal corresponding author

*Email address:* phopkins@virginia.edu (Patrick E. Hopkins)

## Contents

<b>1</b>	<b>High resolution x-ray diffraction (HRXRD) measurements</b>	<b>3</b>
1.1	(111) HRXRD measurements, RADS simulations . . . . .	3
<b>2</b>	<b>Plan-view scanning electron microscopy (SEM)</b>	<b>4</b>

# 1. High resolution x-ray diffraction (HRXRD) measurements

## 1.1. (111) HRXRD measurements, RADS simulations

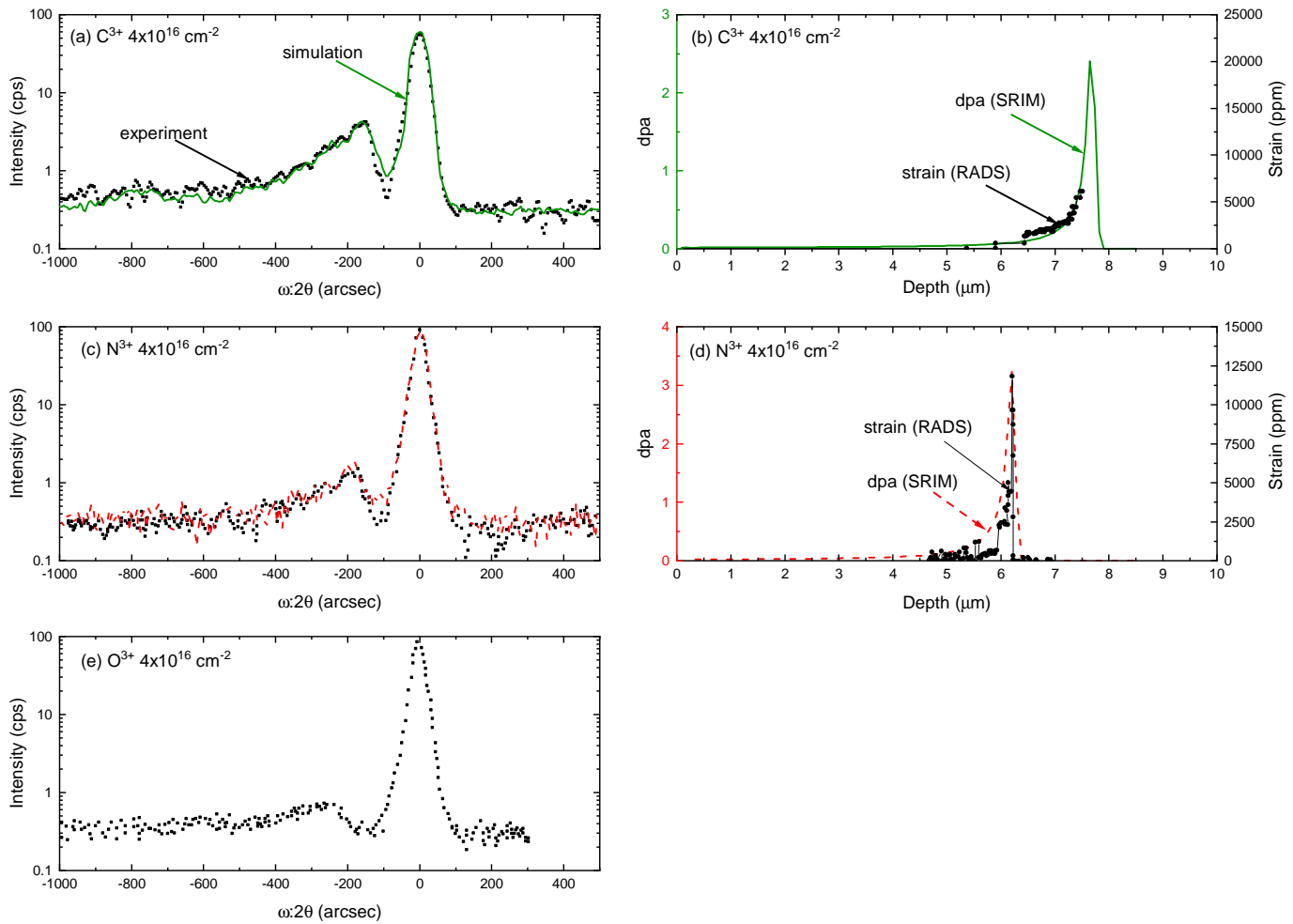


Figure 1: HRXRD measurements of the (111) peak (a,c,e), and corresponding RADS simulations of sample strain (b,d). In (a), (c), and (e), the experimental HRXRD data is represented by black squares, the lines plotted atop the experimental data display the RADS model of the data, from which the strain is simulated. For comparison, the dpa (calculated via SRIM), is plotted along with the strain in (b) and (d); in each case, there is negligible strain expected prior to the end of range. The strain intensity for the  $\text{O}^{3+}$  implanted sample was found to be too low to adequately model with RADS, and therefore a strain profile could not be generated.

## 2. Plan-view scanning electron microscopy (SEM)

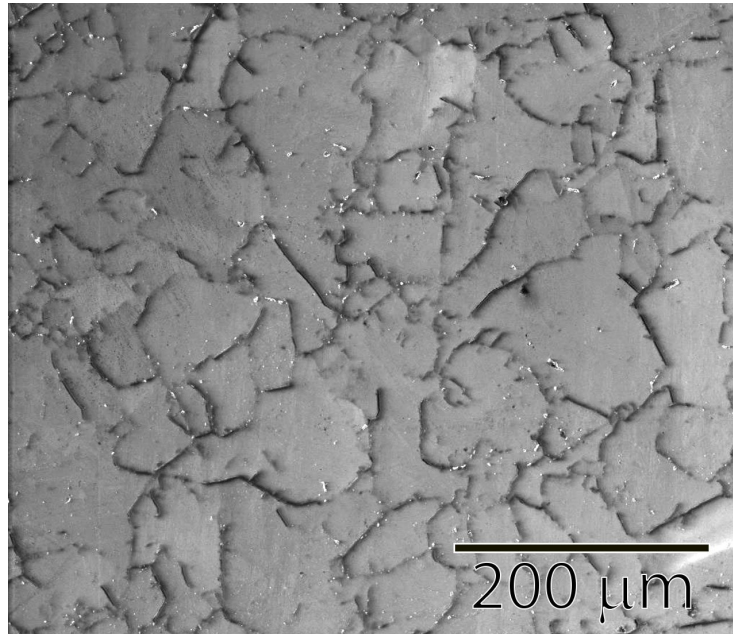


Figure 2: Plan view SEM image of the surface of a diamond wafer. The dark lines, indicating grain boundaries, suggest that grains within the material are on the order of tens of  $\mu\text{m}$ , consistent with other measurements of grain size of polycrystalline CVD grown synthetic diamonds in the literature [1, 2, 3]. From kinetic theory approximation ( $\kappa = 1/3C_v v l$  where  $\kappa$  is thermal conductivity,  $C_v$  is volumetric heat capacity,  $v$  is sound speed in the material, and  $l$  is phonon mean free path), the mean free path is found to be  $0.28 \mu\text{m}$ , when using the unirradiated thermal conductivity ( $1,996 \text{ W m}^{-1} \text{ K}^{-1}$ ), and taking the volumetric heat capacity and sound speed as  $1.78 \times 10^6 \text{ J m}^{-3} \text{ K}^{-1}$  and  $12,000 \text{ m s}^{-1}$ , respectively. This suggests that from a thermal perspective, the sample can be considered as bulk.

## References

- [1] F. Sun, Y. Ma, B. Shen, Z. Zhang, M. Chen, Fabrication and application of nano-microcrystalline composite diamond films on the interior hole surfaces of Co cemented tungsten carbide substrates, *Diamond and Related Materials* 18 (2-3) (2009) 276–282. doi:10.1016/j.diamond.2008.10.064.  
URL <http://dx.doi.org/10.1016/j.diamond.2008.10.064>
- [2] J. E. Graebner, S. Jin, G. W. Kammlott, J. A. Herb, C. F. Gardinier, Large anisotropic thermal conductivity in synthetic diamond films, *Nature* 359 (6394) (1992) 401–403. doi:10.1038/359401a0.
- [3] M. Zhang, Y. Xia, L. Wang, B. Gu, Effects of the grain size of CVD diamond films on the detector performance, *Journal of Materials Science* 40 (19) (2005) 5269–5272. doi:10.1007/s10853-005-0737-1.